SLAC-PUB-16830

Self-referenced coherent diffraction x-ray movie of Ångstrom- and femtosecond-scale atomic motion

J. M. Glownia,[1,2,*] A. Natan,[2,*] J. P. Cryan,[2] R. Hartsock,[2] M. Kozina,[1] M. P. Minitti,[1] S. Nelson,[1] J. Robinson,[1] T. Sato,[1] T. van Driel,[1] G. Welch,[1] C. Weninger,[2,1] D. Zhu,[1] and P. H. Bucksbaum[2,3]

[1]*Linac Coherent Light Source, SLAC National Accelerator Laboratory, Menlo Park, CA 94025*
[2]*Stanford PULSE Institute, SLAC National Accelerator Laboratory Menlo Park, CA 94025*
[3]*Departments of Physics, Applied Physics, and Photon Science, Stanford University, Stanford, CA 94305.*

(Dated: September 29, 2016)

Time-resolved femtosecond x-ray diffraction patterns from laser-excited molecular iodine are used to create a movie of intramolecular motion with a temporal and spatial resolution of 30 fs and 0.3 Å. This high fidelity is due to interference between the non-stationary excitation and the stationary initial charge distribution. The initial state is used as the local oscillator for heterodyne amplification of the excited charge distribution to retrieve real-space movies of atomic motion on Ångstrom and femtosecond scales. This x-ray interference has not been employed to image internal motion in molecules before. Coherent vibrational motion and dispersion, dissociation, and rotational dephasing are all clearly visible in the data, thereby demonstrating the stunning sensitivity of heterodyne methods.

High brightness ultrafast hard x-ray free electron lasers (FELs) can perform time-resolved x-ray diffractive imaging. Recent demonstrations of time-resolved crystal diffraction or time-resolved non-periodic imaging illustrate the power of these sources to track Ångstrom-scale motion [1, 2]. These have spurred new insights in broad areas of science, but have not fully realized the potential of x-ray FELs to image molecules with simultaneous sub-Ångstrom and few-femtosecond resolution. Previous x-ray or electron scattering experiments have used correlations between simulations and data to extract femtosecond molecular dynamics information [3–7].

Here we propose and demonstrate an imaging method that employs a universal but unappreciated feature of time-resolved hard x-ray scattering that dramatically improves reconstructed images of charge motion, and enables femtosecond and sub-Ångstrom x-ray movies. The method relies on the "pump-probe" protocol, where motion is initiated by a short "start" pulse, and then interrogated at a later time by a "probe" pulse. The pumped fraction is small, and the unexcited fraction is our heterodyne reference [8].

When a gas of N identical molecules in a thermal distribution is excited with probability a from the ground state g to an excited state e, only a fraction aN molecules are in e but there is no information about which ones. If we scatter x-rays from this system, the elastic scattering amplitude [9]

$$f(\vec{Q},t) = \int d^3x \rho(\vec{x},t) e^{i\vec{Q}\cdot\vec{x}}, \tag{1}$$

is the normalized sum of $f^{(g)}$ or $f^{(e)}$ from all N molecules in all M possible excitation configurations. Here ρ is the instantaneous charge density, $\vec{Q}$ is the photon momentum transfer, and $M = \binom{N}{aN} = N!/[(N-aN)!aN!]$. This sum can be expanded:

$$f(\vec{Q}) = (1/M)\sum_{i=1}^{M}\left[\sum_{j=1}^{aN} f_{ij}^{(e)}(\vec{Q}) + \sum_{j=1}^{(1-a)N} f_{ij}^{(g)}(\vec{Q})\right]. \tag{2}$$

The order of summing can be re-arranged so that the factor $1/M$ cancels the sum over $i = 1, M$, leaving:

$$f(\vec{Q}) = \sum_{j=1}^{N}\left[a f_j^{(e)}(\vec{Q}) + (1-a) f_j^{(g)}(\vec{Q})\right] \tag{3}$$

The square of this amplitude is the intensity on the detector. Cross terms between different molecules average out due to their random position in the gas, so the scattered intensity I is linear in the number of molecules N:

$$I(\vec{Q}) = |f(\vec{Q})|^2 = N|a f^{(e)}(\vec{Q}) + (1-a) f^{(g)}(\vec{Q})|^2 \tag{4}$$

This signal is an incoherent sum of the coherent diffraction from each molecule. Such a system is described by a quantum density matrix for coherent rovibrational excitation with incoherent mixtures of ground and excited electronic states. Eq.4 differs from the result for an inhomogeneous gas mixture where there are no intramolecular cross terms and the intensity distributions of the two species simply add.

The key insight in Eq.4 is that scattering from the excited fraction in each molecule interferes with scattering from its initial state fraction, producing holographic fringes. The scattering from the excitation alone without ground-state interference goes as a^2N according to Eq. 4; but the modulation due to holographic interference has a peak-to-peak amplitude proportional to $4aN$. This increase factor of $4/a$ in the pattern of x-rays on the detector makes it possible to create high fidelity images of the excited charge distribution using heterodyne deconvolution to extract the signal.

This material is based upon work supported by the U.S. Department of Energy, Office of Science, under Contract No. DE-AC02-76SF00515.

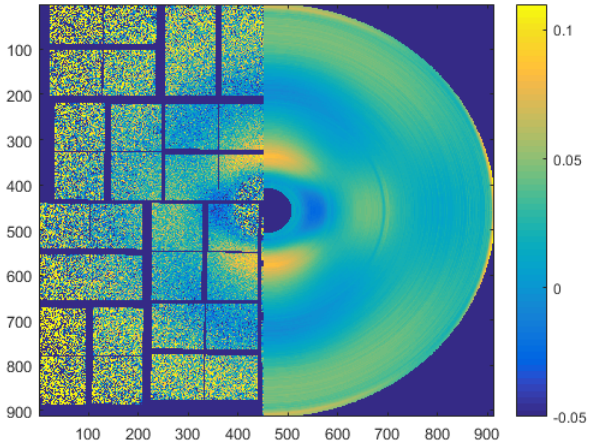

FIG. 1. Left: Half of the LCLS 2.5 megapixel array detector (CSPAD [20]) showing the fractional deviation from the mean scattering signal recorded in each pixel at a pump-probe delay of 150 fs, integrated over 100 x-ray pulses. Right: The Legendre polynomial fit obtained by applying Eq. 5 to the data at this time delay. The scattering vs. time delay appears as a movie in Supplemental Material [21].

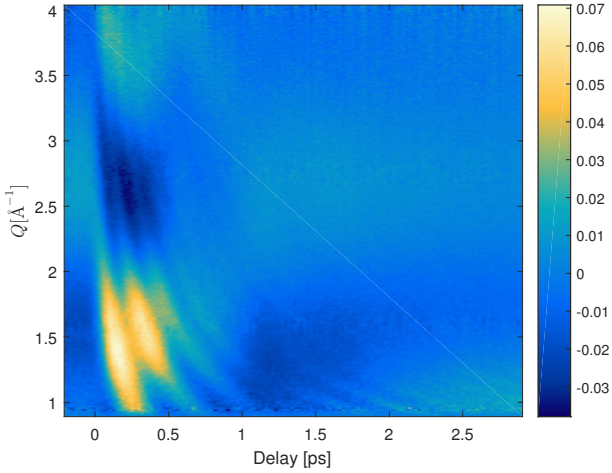

FIG. 2. $\beta_2(Q,t)$ as defined in Eq. 5. This term captures most of the excited state scattering signal. The time-averaged value is subtracted, and the scale is the fraction of modulation due to the holographic interference between the excited state and the reference ground state. The principal features are long-period oscillations in Q that are due to the B state, and much shorter period oscillations in Q caused by dissociation.

Formal descriptions of time-resolved x-ray diffraction in small molecules have not discussed the importance of this self-referenced interference [9–16]. Eq. 4 has been noted previously, but has not been implemented for molecular movies [16–19]. The initial reference distribution is extracted from negative delay data, when the probe sees the initial distribution. The deconvolved signal is a *de-novo* molecular movie.

A demonstration of coherent self-referenced time-resolved imaging was performed at the X-ray Pump Probe (XPP) facility at the Linac Coherent Light Source (LCLS) [22]. Molecular iodine vapor was resonantly excited with a short laser pulse from the X($^1\Sigma_g^+$) state to the B($^3\Pi_{0u}^+$) state [23]. This excites a coherent vibrational wavepacket [24].

We apply a standard correction to remove the effect of the angle dependence of the Thomson scattering cross section in the horizontal scattering plane due to the LCLS linearly polarized x rays, and we rebin in (Q,θ) coordinates. Data from each radial value are fit to a Legendre polynomial basis (Fig.1)

$$I(Q,\theta,t) = A(Q,t)\left[1+\sum_{n=1}^{3}\beta_{2n}(Q,t)P_{2n}(\cos(\theta))\right] \quad (5)$$

The apparatus for gas phase scattering has been described previously [25]. The pump pulse (520 ± 5 nm, 20 μJ, 120 Hz, 50 fs, vertical polarization, 100μm beam diameter) was created by an optical parametric amplifier. The probe pulse (9.0 keV, 2 mJ, 120 Hz, 40 fs, horizontal polarization, 30μm beam diameter) was a spatially coherent beam of x-rays provided by the LCLS. The co-propagating cross-polarized beams were focused into a windowless iodine cell inside a larger vacuum enclosure with a sapphire/beryllium output window. The perpendicular beam polarizations ensure that the B-state modulation is in a direction where the x-ray scattering cross section is insensitive to angle. The cell was heated to 100° C, with a column density of $\sim 10^{18}$ cm^{-2}. The photoexcitation fraction of ∼10% depends on the photon fluence, attenuation length, beam overlap, and the wavelength-dependent cross section [26]. The X-ray attenuation was 50% from transmission losses and 8% from iodine photoabsorption. Approximately 0.4% of the remaining x rays undergo iodine elastic scattering, and 2% of these (10^7 x rays per pulse) scatter at angles that intercept the 2.3 megapixel silicon array (Cornell-SLAC Pixel Array Detector [20]) detector. Up to 50 scattered x-rays per pulse per pixel were detected.

The x-ray scattering amplitude in Eq.1 depends on the instantaneous charge density $\rho(\vec{x},t)$ [9]. Most of the 53 electrons in iodine are in core orbitals, so the x-rays scatter primarily from the vicinity of the atomic nuclei, and thus the time-dependent charge density will approximately follow the rovibrational motion of the molecule. Before excitation all of the iodine molecules are in a thermal state in the X manifold. The laser pulse creates electronically excited rovibrational wavepackets, mostly on the B-state. A typical example of the fractional change in the x-ray diffraction pattern due to laser excitation is shown in Fig. 1. The data were discriminated based on x-ray beam parameters (bunch charge, photon energy,

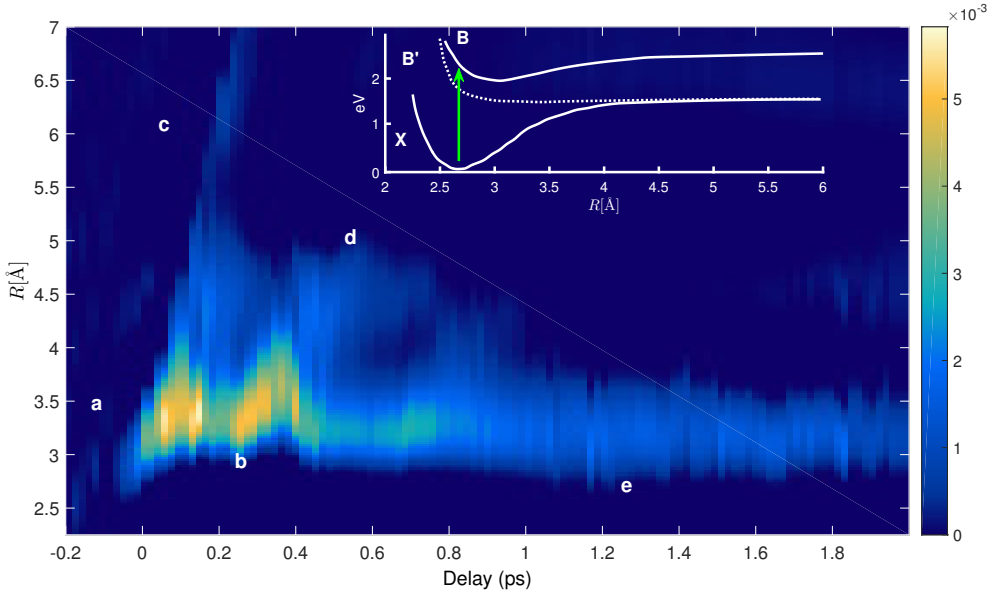

FIG. 3. Extracted excited-state charge distribution vs time, for R from 2.3 to 7 Å and time delays out to 2 ps. This "movie" was extracted from $\beta_2(Q,t)$ (see Fig. 2) using Eqns. 1-9. Bound-state wavepacket oscillations, dissociation, and rotational dephasing are clearly visible. Letters refer to features described in the text. The scale is proportional to the excitation in the β_2 channel. Inset: Excitation path and iodine molecular potentials. A video is in Supplemental Material [21].

pulse energy, and beam position).

Only the even Legendre polynomials are used because the geometry cannot break the up/down symmetry of the molecular ensemble. Contributions for $n > 3$ are negligible.

The radial modulations in Fig. 1 are captured in the $\beta_2(Q,t)$ coefficient of Eq. 5, plotted in Fig. 2. This picks out scattering patterns with the symmetry of an electric dipole excitation, and contains nearly all of the time-varying portion of the total scattered signal. The large-amplitude modulations in Fig.2 are due to holographic interference between the nonstationary charge distribution of the laser-excited wavepacket and the stationary initial charge distribution. Heterodyne techniques described below allow us to deconvolve the excitation in space and plot it vs. time in Fig. 3 as a movie with femtosecond and Ångstrom resolution.

For time delays $t < 0$ the x-rays scatter from the iodine before the exciting laser arrives in the sample, and therefore the distribution is stationary and contained in the isotropic $A(Q,t)$ portion of Eq. 5.

The features in the movie that follow the excitation pulse at t=0 reveal the detailed quantum evolution of this system. The letters at the beginning of the following paragraphs refer to labeled areas of Fig. 3.

(a) A region of approximately 100 fs (about five discrete pump-probe delay points) around $t = 0$ shows where the excited state activity begins. The Franck Condon region, where the B-state is directly over the X-state, is centered around 2.7 Å in iodine. Charge appears across this region moving rapidly towards the center of the B-state potential at approximately 3 Å and then moving beyond towards the outer turning point, approximately 4.5 Å for this excitation wavelength.

(b) The vibrational oscillations in bound states in the molecule can be observed in some detail. See also wavepacket simulations in Supplementary Material [21]. The excitation is spread over several hundred cm^{-1} (~ 40 meV) by thermal broadening of the initial state. The wave packet is high in the anharmonic portion of the B-state potential, and the bound motion in the B-state appears highly dispersed [24, 27].

(c) There is a pulse of dissociating charge that starts near $(R,t) = (2.7$ Å, $0)$ and moves rapidly away from the bound region with constant velocity and only 4% of the total excited charge. The fringes recorded in Fig. 2 are sufficiently fine to show that this feature has little dispersion out to at least 16Å, well beyond the range included in Fig. 3. Its velocity is 16 Å/ps, corresponding to a kinetic energy release of approximately 0.85 eV, consistent with the separation velocity required for the molecule to dissociate into two ground-state atoms for our excitation wavelength. This prompt dissociation is consistent with transitions to a family of repulsive *ungerade* states, one of which is shown in the inset in Fig. 3 [23, 28].

(d) Local moving peaks in the charge density are observed near the outer turning point at time delays of 0.5-0.7 ps. Similar cusp-like features are predicted but have not been observed directly before [24, 27]. See simulation in Supplemental Material [21].

(e) The mean position of the excited population reaches a minimum value of 3 Å near 1.2 ps. This is consistent with rotational dephasing of the $\cos^2\theta$ alignment created in the excited state. For iodine at 100° C the initial prolate alignment along $\hat{z}$ evolves to a nearly isotropic distribution at 1.2 ps [29–31] in agreement with the data in Fig. 3. Rotational dephasing also affects the total amount of charge vs. time in Fig. 3. The amplitude decreases as population moves from $\cos^2\theta$ to a more isotropic distribution. Beyond the point of minimum alignment at 1.2 ps the signal is only about 1/3 the initial strength. See simulation in Supplemental Material [21].

The method used to "invert" this scattering image uses the heterodyne beating that is evident in figure 2. Below we describe the step-by-step procedure for obtaining the movie in Fig. 3.

The charge density $\rho(\vec{x},t)$ that appears in Eq. 1 is the expectation value of the charge density operator in the $|\vec{x}>$ basis, which is the trace of the density matrix over the electronic coordinates multiplied by the electron charge. This can be divided into an initial charge distribution $\rho_0(\vec{x})$ and a time-varying distribution $\rho_e(\vec{x},t)$ without loss of generality. This agrees with Eq. 4 for the x-ray intensity $I(\vec{Q},t) = \left|f(\vec{Q},t)\right|^2$.

We approximate $\rho_0(\vec{x})$ in the analysis by $\rho(\vec{x},t<0)$, the charge distribution before the laser excitation. The object of the analysis is to discover $\rho_e(\vec{x},t>0)$, and thereby create a molecular movie. The precise form of the time-independent initial distribution is easily calculated, but we stress here that its most important feature is that it serves as a time-independent reference in the time-varying scattering pattern in a pump-probe experiment.

The process of extracting the excitation from the measured scattering pattern uses heterodyne deconvolution. The first step is a 2-dimensional inverse Fourier transform of the scattering image. This cannot recover the charge distribution directly because the scattering is the squared Fourier transform and therefore has no phase information. However this is an autocorrelation of the charge distribution:

$$\mathcal{FT}^{-1}_{2D}(f(\vec{Q},t)f^*(\vec{Q},t)) = \mathcal{AC}[\rho(\vec{x},t)] \equiv \rho(\vec{x},t)\otimes\rho(\vec{x},t) \qquad (6)$$

The right side of Eq. 6 has contributions from the time-independent reference and the smaller time-dependent wave packet:

$$\mathcal{AC}[\rho(\vec{x},t)] = \mathcal{AC}[\rho_0(\vec{x})] + \mathcal{AC}[\rho_e(\vec{x},t)] + 2\mathcal{CC}[\rho_0(\vec{x}),\rho_e(\vec{x},t)] \qquad (7)$$

Here $\mathcal{CC}$ is a convolution integral (i.e. cross-correlation) $\mathcal{CC}[\rho_0(\vec{x}),\rho_e(\vec{x},t)] = \rho_0(\vec{x})\otimes\rho_e(\vec{x},t)$. The first term in Eq. 7 on the right side is obtained from the $t<0$ measurements and can be subtracted. The second term is second order in the excitation fraction, and may be neglected if the excitation is small. We then obtain:

$$2\,\mathcal{CC}[\rho_0(\vec{x}),\rho_e(\vec{x},t)] \simeq \mathcal{AC}[\rho(\vec{x},t)] - \mathcal{AC}[\rho_0(\vec{x})] \qquad (8)$$

The final step to produce a molecular movie uses the convolution theorem once more to extract $\rho_e(\vec{x},t)$:

$$\rho_e(\vec{x},t) = \mathcal{FT}^{-1}_{2D}\left[\frac{\mathcal{FT}_{2D}(\mathcal{CC}[\rho_0(\vec{x}),\rho_e(\vec{x},t)])}{\mathcal{FT}_{2D}[\rho_0(\vec{x})]}\right]. \qquad (9)$$

In this step the initial charge distribution $\rho_0(\vec{x})$ is approximated as the thermal population of levels of the X-state:

$$\rho_0(\vec{x}) \sim \rho_X(\vec{x}) = \sum_{v=0}^{\infty}\rho_v(\vec{x})e^{-E_v/k_BT}. \qquad (10)$$

This is a compact point-spread function for deconvolution in Eq. 9. The image retrieval is thus similar to deblurring in microscopy. We project Eq. 8 onto $P_2(\cos\theta)$ and perform a deconvolution (Lucy-Richardson) along R, yielding Fig. 3. This deconvolution is robust for several standard algorithms. The resulting resolution is already comparable to the limits in Q imposed by counting statistics and our scattering geometry.

Self-referencing should be applicable to many small molecules in liquid or gas phase. The requirements are: good statistics since the excitation fraction is small; Sufficient Q-resolution to resolve single bonds; and some knowledge of the initial state charge distribution. It could be valuable for photo-initiated molecular energy conversion studies such as thymine photoprotection, retinal isomerization, and cyclohexadiene ring openings, providing molecular movies at the single bond level with relevant time resolution. Pre-alignment methods can improve the measurement fidelity. Since x-ray scattering only detects charge density and motion, it cannot measure electron energies or spins. Complementary information comes from time-resolved electron and x-ray spectroscopies and photoelectron imaging [32–34].

Future higher energy and higher repetition rate x-ray FELs could increase the fidelity and resolution of molecular movies. Likewise, the method could be used equally well with sub-femtosecond x-ray pulses, or with enhanced harmonic radiation from FEL undulators.

We wish to acknowledge useful discussions with Ryan Coffee, Markus Guehr, Lucas Zipp, Andreas Kaldun, Jerry Hastings, Kelly Gaffney, Bob Schoenlein, and David Reis in the preparation of this paper. This research is supported through the Stanford PULSE Institute, SLAC National Accelerator Laboratory by the U.S. Department of Energy, Office of Basic Energy Sciences, Atomic, Molecular, and Optical Science Program. Use of the Linac Coherent Light Source (LCLS), SLAC National Accelerator Laboratory, is supported by the U.S. Department of Energy, Office of Science, Office of Basic Energy Sciences under Contract No. DE-AC02-76SF00515.

* J.M. Glownia and A. Natan contributed equally to this work.

[1] M. Trigo, M. Fuchs, J. Chen, M. P. Jiang, M. Cammarata, S. Fahy, D. M. Fritz, K. Gaffney, S. Ghimire, A. Higginbotham, S. L. Johnson, M. E. Kozina, J. Larsson, H. Lemke, A. M. Lindenberg, G. Ndabashimiye, F. Quirin, K. Sokolowski-Tinten, C. Uher, G. Wang, J. S. Wark, D. Zhu, and D. A. Reis, Nature Physics **9**, 790 (2013).

[2] C. Kupitz, S. Basu, I. Grotjohann, R. Fromme, N. A. Zatsepin, K. N. Rendek, M. S. Hunter, R. L. Shoeman, T. A. White, D. Wang, D. James, J.-H. Yang, D. E. Cobb, B. Reeder, R. G. Sierra, H. Liu, A. Barty, A. L. Aquila, D. Deponte, R. A. Kirian, S. Bari, J. J. Bergkamp, K. R. Beyerlein, M. J. Bogan, C. Caleman, T.-C. Chao, C. E. Conrad, K. M. Davis, H. Fleckenstein, L. Galli, S. P. Hau-Riege, S. Kassemeyer, H. Laksmono, M. Liang, L. Lomb, S. Marchesini, A. V. Martin, M. Messerschmidt, D. Milathianaki, K. Nass, A. Ros, S. Roy-Chowdhury, K. Schmidt, M. Seibert, J. Steinbrener, F. Stellato, L. Yan, C. Yoon, T. A. Moore, A. L. Moore, Y. Pushkar, G. J. Williams, S. Boutet, R. B. Doak, U. Weierstall, M. Frank, H. N. Chapman, J. C. H. Spence, and P. Fromme, Nature **513**, 261 (2014).

[3] M. Minitti, J. Budarz, A. Kirrander, J. Robinson, D. Ratner, T. Lane, D. Zhu, J. Glownia, M. Kozina, H. Lemke, M. Sikorski, Y. Feng, S. Nelson, K. Saita, B. Stankus, T. Northey, J. Hastings, and P. Weber, Physical Review Letters **114**, 255501 (2015).

[4] J. Küpper, S. Stern, L. Holmegaard, F. Filsinger, A. Rouze, A. Rudenko, P. Johnsson, A. V. Martin, M. Adolph, A. Aquila, S. Bajt, A. Barty, C. Bostedt, J. Bozek, C. Caleman, R. Coffee, N. Coppola, T. Delmas, S. Epp, B. Erk, L. Foucar, T. Gorkhover, L. Gumprecht, A. Hartmann, R. Hartmann, G. Hauser, P. Holl, A. Hmke, N. Kimmel, F. Krasniqi, K.-U. Khnel, J. Maurer, M. Messerschmidt, R. Moshammer, C. Reich, B. Rudek, R. Santra, I. Schlichting, C. Schmidt, S. Schorb, J. Schulz, H. Soltau, J. C. Spence, D. Starodub, L. Strder, J. Thgersen, M. J. Vrakking, G. Weidenspointner, T. A. White, C. Wunderer, G. Meijer, J. Ullrich, H. Stapelfeldt, D. Rolles, and H. N. Chapman, Physical Review Letters **112**, 083002 (2014).

[5] J. Yang, M. Guehr, T. Vecchione, M. S. Robinson, R. Li, N. Hartmann, X. Shen, R. Coffee, J. Corbett, A. Fry, and et al., Nature Communications **7**, 11232 (2016).

[6] C. I. Blaga, J. Xu, A. D. DiChiara, E. Sistrunk, K. Zhang, P. Agostini, T. A. Miller, L. F. DiMauro, and C. D. Lin, Nature **483**, 194 (2012).

[7] R. Boll, D. Anielski, C. Bostedt, J. D. Bozek, L. Christensen, R. Coffee, S. De, P. Decleva, S. W. Epp, B. Erk, and et al., Physical Review A **88**, 61402 (2013).

[8] B. Wu, Y. Liu, C. Rose-Petruck, and G. J. Diebold, Applied Physics Letters **100**, 61110 (2012).

[9] G. Dixit, O. Vendrell, and R. Santra, Proceedings of the National Academy of Sciences **109**, 1163611640 (2012).

[10] M. Ben-Nun, J. Cao, and K. R. Wilson, The Journal of Physical Chemistry A **101**, 87438761 (1997).

[11] J. Cao and K. R. Wilson, The Journal of Physical Chemistry A **102**, 9523 (1998), http://dx.doi.org/10.1021/jp982054p.

[12] S. Bratos, F. Mirloup, R. Vuilleumier, and M. Wulff, The Journal of Chemical Physics **116**, 10615 (2002).

[13] N. E. Henriksen and K. B. Møller, The Journal of Physical Chemistry B **112**, 558 (2008), pMID: 18052363, http://dx.doi.org/10.1021/jp075497e.

[14] U. Lorenz, K. B. Møller, and N. E. Henriksen, Phys. Rev. A **81**, 023422 (2010).

[15] A. Debnarova, S. Techert, and S. Schmatz, The Journal of Chemical Physics **133**, 124309 (2010).

[16] M. Ben-Nun, T. J. Martnez, P. M. Weber, and K. R. Wilson, Chemical Physics Letters **262**, 405414 (1996).

[17] M. Woerner, F. Zamponi, Z. Ansari, J. Dreyer, B. Freyer, M. Prmont-Schwarz, and T. Elsaesser, The Journal of Chemical Physics **133**, 64509 (2010).

[18] M. J. J. Vrakking and T. Elsaesser, Nature Photonics **6**, 645647 (2012).

[19] D. A. Reis and A. M. Lindenberg, "Ultrafast x-ray scattering in solids," in *Light Scattering in Solid IX*, Topics in Applied Physics, edited by M. Cardona and R. Merlin (Springer Berlin Heidelberg, 2006) p. 371422.

[20] S. Herrmann, S. Boutet, B. Duda, D. Fritz, G. Haller, P. Hart, R. Herbst, C. Kenney, H. Lemke, M. Messerschmidt, *et al.*, Nuclear Instruments and Methods in Physics Research Section A: Accelerators, Spectrometers, Detectors and Associated Equipment **718**, 550 (2013).

[21] See Supplemental Material at [URL will be inserted by publisher] for movies and simulations related to this experiment.

[22] M. Chollet, R. Alonso-Mori, M. Cammarata, D. Damiani, J. Defever, J. T. Delor, Y. Feng, J. M. Glownia, J. B. Langton, S. Nelson, and et al., Journal of Synchrotron Radiation **22**, 503507 (2015).

[23] J. Tellinghuisen, The Journal of Chemical Physics **59**, 849852 (1973).

[24] J. L. Krause, R. M. Whitnell, K. R. Wilson, Y. Yan, and S. Mukamel, The Journal of Chemical Physics **99**, 65626578 (1993).

[25] J. M. Budarz, M. P. Minitti, D. V. Cofer-Shabica, B. Stankus, A. Kirrander, J. B. Hastings, and P. M. Weber, Journal of Physics B: Atomic, Molecular and Optical Physics **49**, 34001 (2016).

[26] A. Saiz-Lopez, R. W. Saunders, D. M. Joseph, S. H. Ashworth, and J. M. C. Plane, Atmos. Chem. Phys. **4**, 14431450 (2004).

[27] H. Chen, L. Fang, V. Tagliamonti, and G. N. Gibson, Physical Review A **84**, 43427 (2011).

[28] **55**, 10.1063/1.1675521.

[29] D. W. Broege, R. N. Coffee, and P. H. Bucksbaum, Physical Review A **78**, 35401 (2008).

[30] F. Rosca-Pruna and M. J. J. Vrakking, The Journal of Chemical Physics **116**, 65796588 (2002).

[31] F. Rosca-Pruna and M. J. J. Vrakking, Physical Review Letters **87**, 153902 (2001).

[32] A. Stolow, A. E. Bragg, and D. M. Neumark, Chem. Rev. **104**, 1719 (2004).

[33] T. Suzuki, Annual Review of Physical Chemistry **57**, 555 (2006).

[34] B. K. McFarland, J. P. Farrell, S. Miyabe, F. Tarantelli, A. Aguilar, N. Berrah, C. Bostedt, J. D. Bozek, P. H. Bucksbaum, J. C. Castagna, and et al., Nature Communications **5**, 4235 (2014).

Supplemental Materials: Self-referenced coherent diffraction x-ray movie of Ångstrom- and femtosecond-scale atomic motion

Supplement 1: Raw scattering data movie

A movie showing the raw data as a function of pump-probe delay is shown here. The average scattering image over all time delays has been subtracted so that the interference features can be seen more easily.

Supplement 2: Legendre fit movie

This movie shows the Legendre polynomial fits to the data using Eq.5.

Supplement 3: Molecular movie

Here is a movie rendering of Fig.3 projected onto a $\cos^2\theta$ distribution.

Supplement 4: Simulations

A vibrational wavepacket simulation and rotational dephasing simulation using the experimental parameters are shown here.

Vibrational wavepacket simulation

The probability density of the B-state wavepacket $|\psi_B(R,t)|^2$ excited in this experiment is simulated in Figure S1. The principal differences from the experiment are (1) the model is carried out in the molecular frame so that rotational degrees of freedom are absent and the only relevant parameter is the internuclear separation R between the iodine atoms; (2) only the X and B state manifolds in I_2 are included in the density matrix, so dissociation channels are absent in the simulation; and (3) the excitation is simulated as an idealized transform-limited pulse. The initial charge distribution is a 100° C thermal vibrational ensemble (Eqn. 10). The pump in the model is a 50 fs (FWHM) Gaussian laser pulse with a central wavelength of 520 nm. A split-step method is used to propagate the density matrix in time.

This simulation reproduces the diffuse nature of the wavepacket seen at the outer turning points in Fig.3. In addition, the cusp-like "molecular canon" features at the outer turning point are seen in both the simulation and the experiment. B-state wavepacket oscillations are much more prominent in the simulation than in the experimental result in Fig.3 largely due to the absence of rotational degrees of freedom in the thermal state and the absence of subsequent rotational diffusion, as well as the finite resolution blurring in the experiment. Another factor may be the possible presence of chirp in the excitation pulse, which is not modeled in the simulation.

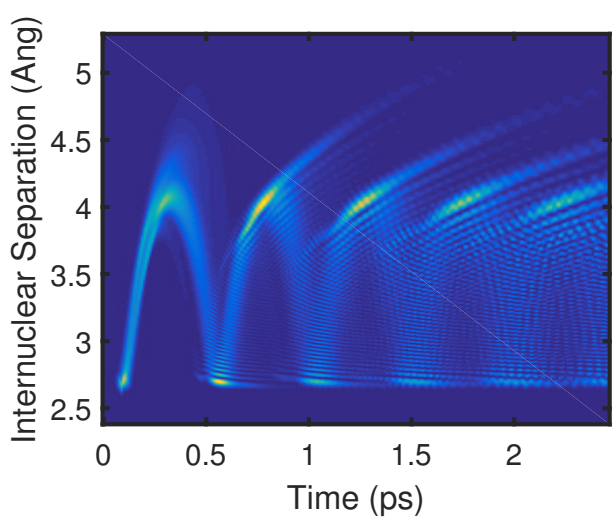

FIG. S1. Simulated vibrational wavepacket in I_2 resulting from the interaction of a thermal (373 K) ground state with a 50 fs laser pulse with central wavelength 520 nm.

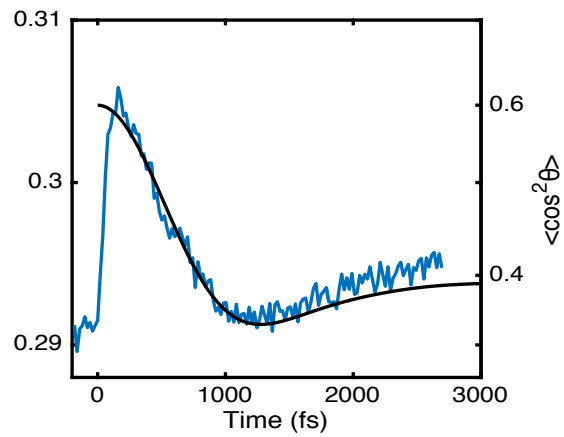

FIG. S2. The projection of Fig 2 onto the time axis, i.e. $\sum_Q \beta_2(Q,t)$ (blue, left axis). The black curve shows the calculated rotational dephasing of the thermal I_2 X-state impulsively projected into a $\cos^2\theta$ distribution (right axis).

Rotational dephasing simulation

Figure S2 shows the projection of the $\beta_2(Q,t)$ coefficient, shown in Fig. 2, onto the Q-axis, $\text{proj}_Q\,[\beta_2] = \sum_Q \beta_2(Q,t)$. The decrease in the projection of the recorded data onto $P_2(\cos^2\theta)$ as a function of time, reaches a minimum near 1.2 ps. We attribute this decrease to rotational dephasing. The minimum in the signal near $t = 1.2$ ps agrees quite well with previous measurements of rotational dephasing time as well as a model calculation of the rotational dephasing of a thermal X-state population projected onto a $\cos^2\theta$ distribution. The dephasing calculation is also shown in Fig. S2.

Size of the β_2 coefficient

Figure S3 shows another representation of the $\beta_2(Q,t)$ coefficient from eqn. 5. Here we show a very coarse time-series and do not perform any mean subtraction. One can see from the figure, that for almost all Q-values and times delays, the value of β_2 is a positive value close to zero, indicating that the excitation is predominatly due to a parallel electric-dipole transition, and the total projection of the data onto $P_2(\cos\theta)$ is rather small. The fast Q-oscillations in the data below $Q = 1.7$ Å^{-1} we attribute to the heterodyne signal from the dissociating wavepacket. The heterodyne signal from the bound B-state wavepacket is seen as larger-period ($T \sim 1.5$ Å^{-1}) Q-oscillations beyond $Q = 1.7$ Å^{-1}.

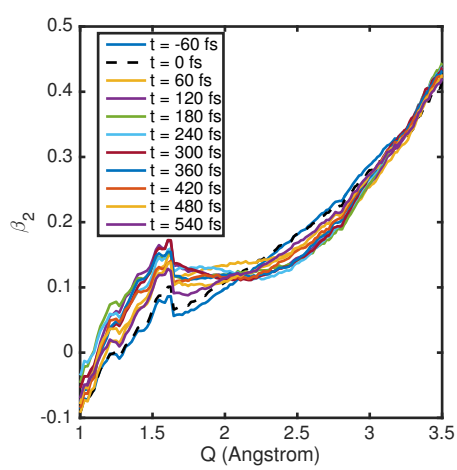

FIG. S3. $\beta_2(Q,t)$ as defined in Eqn. 5, and shown in Fig 2. Here the data is shown without mean subtraction. The heterodyne signal for the B-state wavepacket can be seen in the long-period (~ 1 Å^{-1}) Q-oscillations.

Re: LV14834

Self-referenced coherent diffraction x-ray movie of Angstrom- and femtosecond-scale atomic motion

J. M. Glownia, A. Natan, J. P. Cryan, et al.

To the Editors:

We appreciate the very rapid turnaround of our manuscript, and have tried to respond to the many pages of detailed Referee comments with equal speed.

We have used Supplementary Material to include additional material in response to the reviewers without lengthening the paper.

We have uploaded three movies. The first movie shows the scattering data vs. time delay between molecular excitation and the x-ray probe. The second movie shows this same scattering data following a fit to a Legendre polynomial basis. The third movie is a video rendering of the molecular motion extracted from the data.

The Supplementary Material also includes two simulations that are not required for the main body of the paper but might help a reader gain additional background about the behavior of iodine when it is excited by a laser. One focuses on vibrational motion and the other on rotational dephasing.

Finally, we include in the Supplementary Material a figure showing cuts through the scattering data that show the interference features of Fig. 2 in different ways.

We feel we have also responded adequately to each of the comments of both referees. Our responses and description of any revisions are included on the following pages.

Best regards,

Phil Bucksbaum

Response to Report of Referee A – LV14834/Glownia ————————————————————————-

1) The left half and the right half of Figure 1 have a very different intensity, meaning that the right half is not simply a fit of what is shown on the left. The experiment and the fit should be plotted on the same scale.

We apologize that evidently this wasn't clear. Actually the right half of fig 1 in the submitted manuscript IS the result of a fit of the left half to a series of Legendre polynomials. These average out the high spatial frequency random speckle.

As for the units: Please forgive the misimpression that the scale is arbitrary, since it isn't arbitrary but also isn't explained well. The scale refers to the left half of the figure, which displays the net change in the number read out by the CSPAD detector per pixel due to the laser excitation, integrated over 100 x-ray pulses. Thus the brightest pixels have according the the scale 60 additional units, and the darkest pixels have 40 fewer units. At our x-ray photon energy and the gain value used in the experiment, one detected x-ray registers 27 units. The right half is a fit as described in the text and the caption. Its scale is in the dimensionless units of the normalized fit, but follows the same linear intensity scale.

In response to this comment we will avoid the misimpression that the left and right halves of this figure are somehow different by plotting a percentage deviation rather than absolute counts on the detector.

Revised caption: "Left: Half of the LCLS 2.5 megapixel array detector (CSPAD [S20]) showing the fractional deviation from the mean scattering signal recorded in each pixel at a pump-probe delay of 150 fs, integrated over 100 x-ray pulses. Right: The Legendre polynomial fit obtained by applying Eq. 5 to the data at this time delay. The scattering vs. time delay appears as a movie in Supplementary Material."

2) The authors say diffract before destroy ... Assuming an x-ray spotsize of 10-100 micron (this number ought to be included ... the vast majority of scattered x-ray photons are scattered by molecules that have never before seen an x-ray photon...

These are good points and we have revised the text as suggested.

Revision: (1) Diffract-before-destroy has been deleted; (2) All the pump laser and x-ray beam and excitation parameters have now been included in one place: "The apparatus for gas phase scattering has been described previously [S25]. The pump pulse (520 ± 5 *nm, 20* μ*J, 120 Hz,* 50 *fs, vertical polarization,* 100μ*m beam diameter) was created by an optical parametric amplifier. The probe pulse (*9.0 *keV,* 2 *mJ,* 120 *Hz,* 40 *fs, horizontal polarization,* 30μ*m beam diameter) was a spatially coherent beam of x-rays provided by the LCLS. The co-propagating cross-polarized beams were focused into a windowless iodine cell inside a larger vacuum enclosure with a sapphire/beryllium output window. The perpendicular beam polarizations ensure that the B-state modulation is in a direction where the x-ray scattering cross section is insensitive to angle. The cell was heated to* 100° *C, with a column density of* $\sim 10^{18}$ cm^{-2}*. The photoexcitation fraction of* $\sim$*10% depends on the photon fluence, attenuation length, beam overlap, and the wavelength-dependent cross section [S26]. The X-ray attenuation was 50% from transmission losses and 8% from iodine photoabsorption. Approximately 0.4% of the remaining x rays undergo iodine elastic scattering, and 2% of these (*10^7 *x rays per pulse) scatter at angles that intercept the 2.3 megapixel silicon array (Cornell-SLAC Pixel Array Detector [S20]) detector. Up to 50 scattered x-rays per pulse per pixel were detected."*

3) The authors say that for t<0 the scattering image is static and that the distribution is described by A(Q,t). As far as I can tell, this is not correct. Elastic scattering of polarized x-rays contains a polarization factor, i.e. the scattering intensity depends on the angle between the polarization and the k-vector of the scattered x-ray (see e.g. Optics Express 18, 5713 (2010)). N.B. The fact that this statement is not correct would appear to be consistent with the fact that a non-zero beta2 remains visible at time delays >1 psec, when the authors know that the distribution is almost isotropic again.

We are puzzled by this but will attempt to respond. Our usage of static means not excited by the laser, and surely we have no disagreement that the molecules are not excited by the laser before the laser pulse arrives. However, the reviewer relates the meaning of static to the polarization dependence of the elastic scattering cross section. We are of course aware of the elastic scattering polarization dependence, and the manuscript already states that we have corrected for it. The correction factor does not depend on the pump-probe delay, and so we apply this correction to every delay in a uniform way. Furthermore, following the standard practice of synchrotron scattering experiments, we have arranged for the x-ray and laser polarizations to be perpendicular precisely because then there is no elastic scattering polarization-dependent cross section in the exciting laser $\hat{k} - \hat{\epsilon}$ plane. We also stated this in the original manuscript, although we did not explain why we did this or why this is generally done.

Finally, the reason that a nonzero signal persists beyond 1 ps is that the excited state still exists, even when rotational dephasing has taken place. The lifetime of the B state is only limited by collisions or fluorescence and is much longer than the maximum time delay in the experiment. In the language of the density matrix, the diagonal terms for the different states that make up the X and B manifolds will persist long after the off-diagonal terms within the different states of the B manifold have decayed to zero.

If the reviewer is confused, then so will be some readers, and so we must change something to try to clear it up. In the revision we replace the word "static" with "stationary." In addition, we have expanded and modified the sentence on the correction for the polarization-dependent cross section. In particular we no longer refer to it as a Thomson correction, since that is a kind of field-specific jargon among the synchrotron scattering community and we should use language that is understood by a broader community.

Revision: In place of "angle-dependent Thomson scattering effect" we have inserted: "We apply a standard correction to remove the effect of the angle dependence of the Thomson scattering cross section in the horizontal scattering plane due to the LCLS linearly polarized x rays..." Also, "static" is replaced by "sationary." In the description of the setup we also write, "The co-propagating cross-polarized beams were focused into a windowless iodine cell inside a larger vacuum enclosure with a sapphire/beryllium output window. The perpendicular beam polarizations ensure that the B-state modulation is in a direction where the x-ray scattering cross section is insensitive to angle."

4) The meaning of Q is only described below equation 5, but at that point Q has already been used numerous times in the text.

We now define Q up front. Its usage is consistent.

Revision: Q is now defined at the first point it appears, in the first column of the paper: "...If we scatter x-rays from this system, the elastic scattering amplitude

$$f(\vec{Q},t) = \int d^3x \rho(\vec{x},t) e^{i\vec{Q}\cdot\vec{x}}, \tag{S1}$$

is the normalized sum of $f^{(g)}$ or $f^{(e)}$ from all N molecules in all M possible excitation configurations. Here ρ is the instantaneous charge density, $\vec{Q}$ is the photon momentum transfer, and M is equal to $\binom{N}{aN} = N!/[(N-aN)!aN!]$. This sum can be expanded..."

5) The story told in connection with Figure 3 would benefit from a comparison with a simulation of the vibrational wavepacket, averaged over the ro-vibrational state population of the initial (ground) state. This is easy to do.

Yes, and there is a very important point here: Namely the experiment is an observation of nature, and therefore contains all of the physics, while simulations generally do not. To respond to this comment we have included B-state simulations in the Supplementary Material in a way that they can be directly compared to the experiment. This will supplement and support the point that the effects of finite temperature, rotational relaxation, non-transform limited excitation pulses, and predissociation all contribute to a rich tapestry of physics that can only be approximately simulated in the calculation, but can be seen with some precision in the data. A comment to this effect with a reference to the supplementary material is now in the text explanation of Fig.3.

Revision: We have added a comment in the text about this: "(b) The vibrational oscillations in bound states in the molecule can be observed in some detail [see also wavepacket simulation in Fig.S1 and the accompanying Supplementary Material]."

We also added a Supplemental section with a simulation and accompanying explanation: "The probability density of the B-state wavepacket $|\psi_B(R,t)|^2$ excited in this experiment is simulated in Figure S1. The principal differences from the experiment are (1) the model is carried out in the molecular frame so that rotational degrees of freedom are absent and the only relevant parameter is the internuclear separation R between the iodine atoms; (2) only the X and B state manifolds in I_2 are included in the density matrix, so dissociation channels are absent in the simulation; and (3) the excitation is simulated as an idealized transform-limited pulse. The initial charge distribution is a 100° C thermal vibrational ensemble (Eqn. 10). The pump in the model is a 50 fs (FWHM) Gaussian laser pulse with a central wavelength of 520 nm. A split-step method is used to propagate the density matrix in time.

This simulation reproduces the diffuse nature of the wavepacket seen at the outer turning points in Fig.3. In addition, the cusp-like "molecular canon" features at the outer turning point are seen in both the simulation and the experiment. B-state wavepacket oscillations are much more prominent in the simulation than in the experimental result in Fig.3 largely due to the absence of rotational degrees of freedom in the thermal state and the absence of

subsequent rotational diffusion, as well as the finite resolution blurring in the experiment. Another factor may be the possible presence of chirp in the excitation pulse, which is not modeled in the simulation. Finally, there is a bias in the experiment introduced by the detector cutoff in Q, which not only limits the resolution but also tends to suppress the amplitude of the lowest wave vector components of the extracted image."

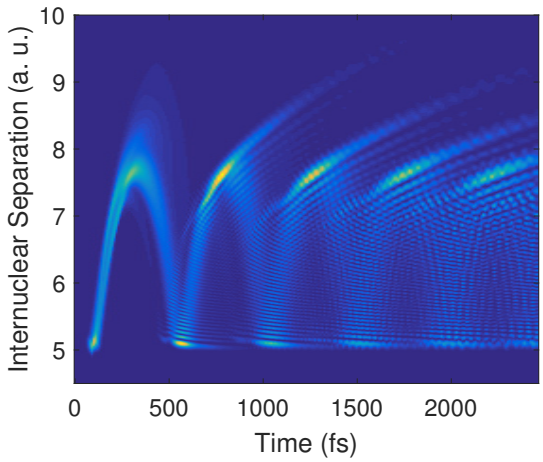

FIG. S1. *Simulated vibrational wavepacket in I_2 resulting from the interaction of a thermal (373 K) ground state with a 50 fs laser pulse with central wavelength 520 nm.*

6) Although not strictly necessary for a proper understanding of the paper, it would be useful for the authors to briefly discuss the relative importance of x-ray scattering involving core and valence electrons.

OK, we have made this change. We already had referred to this in the submitted manuscript when we pointed out that the scattering is mainly from the location of the atoms, but we we have now expanded on that.

Revision: We have added the following to the text: "The x-ray scattering amplitude in Eq.1 depends on the instantaneous charge density $\rho(\vec{x}, t)$ [S9]. Most of the 53 electrons in iodine are in core orbitals, so the x rays scatter primarily from the vicinity of the atomic nuclei, and thus the time-dependent charge density will approximately follow the rovibrational motion of the molecule."

7) In the experiment, the pump laser pulse induces changes in the x-ray scattering image, which are shown in Figure 1. At present the color scale of Figure 1 appears to be in arbitrary units. This color scale should be changed into a scale that relates the measured changes to the intensity of the probe-only image (i.e. a percentage change).

The color scale in Fig. 1 is now in units of fractional change, as requested. The revised figure and caption:

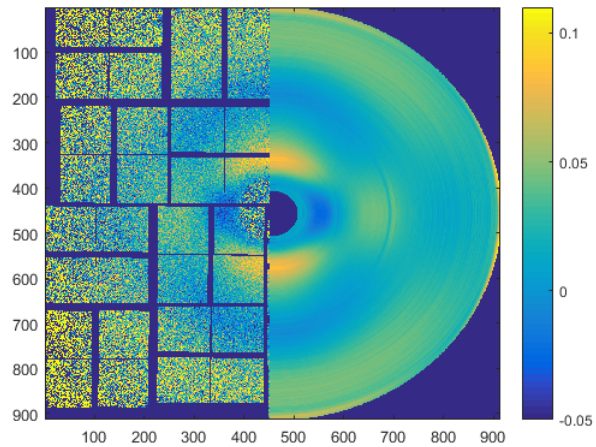

FIG. S2. *Revised Figure 1 and revised caption: Left: Half of the LCLS 2.5 megapixel array detector (CSPAD) showing the fractional deviation from the mean scattering signal recorded in each pixel at a pump-probe delay of 150 fs, integrated over 100 x-ray pulses. Right: The Legendre polynomial fit obtained by applying Eq. 5 to the data at this time delay. The scattering vs. time delay appears as a movie in Supplementary Material.*

8) The physical meaning of the color scale in Figure 3 should be discussed. Presumably the number given for the maximum of the color scale relates to the fraction of excitation in the experiment, but this should be explained.

This value is the measured fractional charge density $\rho(r)$ in the excited state in the β_2 channel, normalized to the total scattering signal over the whole detector. Its value is diluted by noise, imperfect deconvolution, and signal lost to other Legendre polynomial channels, but it should still be a good proportional measure, which is relatively linear.

Revision: We have changed the caption in Fig. 3 to read as follows: "Extracted excited-state charge distribution vs time, for R from 2.3 to 7 Å and time delays out to 2 ps. This "movie" was extracted from $\beta_2(Q,t)$ (see Fig. 2) using Eqns. 1-9. Bound-state wavepacket oscillations, dissociation, and rotational dephasing are clearly visible. Letters refer to features described in the text. The scale is proportional to the excitation in the β_2 channel. Inset: Excitation path and iodine molecular potentials. (A video is in Supplementary Material.)"

Report of Referee B – LV14834/Glownia ——————————————————————-

...I can recommend publishing the manuscript in the Physical Review Letters following revision that I suggest concretely where appropriate... I find that the manuscript does not well distinguish between what is known and what is claimed, what is hypothesized and what is found, what is obvious and what is less obvious or new.

We are certain that this comment is correct. One of Einsteins more famous quotes is "Opinions of obviousness are to a certain extent a function of time." Since we work in a cross-disciplinary field we are constantly confronted with different standards of obviousness between different fields of physics, and these standards evolve rapidly. One of the important functions of these referee reports is to help identify and repair confusion based on this.

I find it hard to assess the size of the effect. I thus suggest thinking about including more (raw) data or data from control experiments that make this accessible. I suggest some ideas that came to my mind below.

In response to this comment and many comments by Referee A we include considerably more raw data. Fig 1 has been revised to display raw data in each pixel for one time delay, and a Supplementary Material section has been added to include a complete movie of the scattering vs. delay.

Revisions: The caption of Fig. 1 now reads: "Left: Half of the LCLS 2.5 megapixel array detector (CSPAD [S20]) showing the fractional deviation from the mean scattering signal recorded in each pixel at a pump-probe delay of 150 fs, integrated over 100 x-ray pulses. Right: The Legendre polynomial fit obtained by applying Eq. 5 to the data at this time delay. [The scattering vs. time delay appears as a movie in Supplementary Material.] "

...I think that the authors need to include some information on the excitation step. What is the fraction of excited molecules?...

We have now addressed this and similar issues.

Revision: We indicate the strength of the interaction of both pump and probe in column 3 of the manuscript: "The photoexcitation fraction of ∼10% depends on the photon fluence, attenuation length, beam overlap, and the wavelength-dependent cross section [S26]. The X-ray attenuation was 50% from transmission and focusing losses and 8% from iodine photoabsorption. Approximately 0.4% of the remaining x rays undergo iodine elastic scattering, and 2% of these (10^7 x rays per pulse) scatter at angles that intercept the 2.3 megapixel silicon array (Cornell-SLAC Pixel Array Detector [S20]) detector."

...vague statement on p. 1 (right column) Even when only 1% of the ensemble is excited,...

This refers to the concept of contrast enhancement in heterodyne methods, which might not be familiar to all scientists. It works like this:

Let us assume that some charge distribution that you would like to image scatters x rays onto your detection screen with intensity S. That signal S is superimposed with a larger background x-ray scattering image R, which we will call the "reference". For example assume that S is much smaller than R so that $S/R = \epsilon$, a small number. The magnitude of the scattering amplitude (i.e. the x-ray electric field) that caused the signal S is $f_S = \sqrt{S}$, and $f_S/f_R = \sqrt{\epsilon}$.

If the x-rays are sufficiently coherent, then the amplitudes can exhibit coherent interference. When f_S and f_R interfere, the peak to peak contrast in the scattering amplitude f is a fraction $\delta f/f = 2\sqrt{\epsilon}$. This means that the total signal $S_tot = f^2$ has peak-to-peak modulation of $(1 \pm \delta f)^2$, or a relative signal size of $4\sqrt{\epsilon}$. For example, a 0.4% relative signal produces a heterodyne beat with a relative peak-to-peak amplitude of nearly 25%. This is the primary reason that heterodyne methods are so valuable: They appear in the total signal as a beat note whose magnitude is proportional to the relative amplitude, not the relative intensity. This simple argument is "obvious" to people in many areas of signal processing science, but different subfields may use different words to describe it.

Revision: We have replaced the vague statement about 1% excitation with an abbreviated version of the previous paragraph in the text.

The new version: "...Eq.4 differs from the result for an inhomogeneous gas mixture where there are no intramolecular cross terms and the intensity distributions of the two species simply add.

"The key insight in Eq.4 is that x-ray scattering from the excited fraction in each molecule interferes with scattering from its initial state fraction, producing holographic fringes. The intensity of the scattered signal from excitation of a small fraction a of the ensemble, considered separately from the reference without any interference effect has size a^2N according to Eq. 4; but the modulation due to holographic interference fringe between the excitation and the ground state has a peak-to-peak amplitude of $4aN$. This amplification factor of $4/a$ in the pattern of x-rays on the detector makes it possible to create high fidelity images of the excited charge distribution..."

Also, following the discussion of feature (c) in Figure 3 (p. 3, left column) it appears eminent to include some information on what is actually excited in the molecule (which states are reached) with the employed wavelength and bandwidth (from known data from literature, from a simulation, from a discussion).

We have now addressed this, in connection also with point 5) of referee A.

Revision: We now include the following information about the general excitation scheme, together with references: "A demonstration of coherent self-referenced time-resolved imaging with ∼ 30 fs and ∼ 0.3Å resolution was performed at the X-ray Pump Probe (XPP) facility at the Linac Coherent Light Source (LCLS) [S22]. Molecular iodine vapor was resonantly excited with a short laser pulse from the ground electronic $X(^1\Sigma_g^+)$ state to the $B(^3\Pi_{0u}^+)$ state [S23]. This excites a coherent vibrational wavepacket [S24].

"The apparatus for gas phase scattering has been described previously [S25]. Briefly, the pump pulse (520 ± 5 nm, 20 μJ, 120 Hz, 50 fs, vertical polarization, 100μm beam diameter) was created by an optical parametric amplifier. The probe pulse (9.0 keV, 2 mJ, 120 Hz, 40 fs, horizontal polarization, 30μm beam diameter) was a highly spatially coherent beam of x-rays provided by the LCLS. The co-propagating cross-polarized beams were focused into a windowless iodine cell inside a larger vacuum enclosure with a sapphire/beryllium output window. The beam polarizations ensure that the B-state modulation is in a direction where the x-ray scattering cross section is insensitive to angle. The cell was heated to 100° C, with a column density of ∼ 10^{18} cm^{-2}. The photoexcitation fraction of ∼10% depends on the photon fluence, attenuation length, beam overlap, and the wavelength-dependent cross section [S26]. The X-ray attenuation was 50% from transmission and focusing losses and 8% from iodine photoabsorption. Approximately 0.4%

of the remaining x rays undergo iodine elastic scattering, and 2% of these (10^7 x rays per pulse) scatter at angles that intercept the 2.3 megapixel silicon array (Cornell-SLAC Pixel Array Detector [S20]) detector. Up to 50 scattered x-rays per pulse per pixel were detected."

Simulations have also been included as Supplementary Material, including vibrational wavepacket simulations as well as separate rotational dephasing simulations. (See also the response to Referee A, point 5)).

In the derivation of Eq. (8), finally, this excitation fraction enters and it appears that it is needed to justify the formalism used to extract the data in Figure 3.

Yes. The small excitation fraction is now addressed, as described in the previous comment response. The excitation fraction enters, but its precise size is not part of the analysis. All that the analysis requires is that the excitation fraction is small.

Revision: See discussion following previous comment.

Understanding that space is limited for manuscripts in the Physical Review Letters I still suggest to include a short discussion of the presented approach in comparison with methods relying on the comparably large cross section of the photoelectric effect. In particular and given the intense and established related research, a comparison with time-resolved photoelectron spectroscopy and with recent initiatives for diffraction from within where structure is determined from photoelectron scattering patterns would be very valuable.

Photoelectron spectroscopy measures electronic structure; here we learn about nuclear structure. Ultrafast electron diffraction (UED), laser-induced electron diffraction (LIED), and photoelectron diffraction (PED) concern the nuclear geometry, and are relevant for comparison. B-state coherent wavepackets in iodine has been studied with TARPES (time- and angle-resolved photoemission) as well as transient photoabsorption, coulomb repulsion imaging, coherent nonlinear spectroscopy, transient birefringence, photoemission and high harmonic generation. This paper is not a review of all this work, nor should it be.

However, the reviewer has a point that a general reader should not have to dig too hard to uncover reports of all of these methods, and so we now refer to some of the more highly cited reports of iodine dynamics.

Revision:

Revison: In the first paragraph we now refer to imaging using electrons as well as x-rays: "Previous x-ray or electron scattering experiments have used correlations between simulations and data to extract femtosecond molecular dynamics information [3-7]"

We have also added a brief discussion and some references on this to the conclusions: "Self-referencing methods for x-ray scattering only detect the density and movement of charge, and cannot address the energy of electron orbitals, or their spins. Complementary information comes from time-resolved electron and x-ray spectroscopies and photoelectron imaging [30-32]".

I find the abstract rather confusing. What is a moving excitation? This x-ray interference suggests that is has been explained in the abstract but, as far as I understand, it only is explained in the following sentence the initial state is used A more conventional step-by-step explanation of what is presented and found would be more accessible to the reader I think.

A re-ordering and slight rephrasing of the sentences in the abstract now addresses this.

Revised abstract to addres these complaints: "Time-resolved femtosecond x-ray diffraction patterns from laser-excited molecular iodine are used to create a movie of intramolecular motion with a temporal and spatial resolution of 30 fs and 0.3 Å. This high fidelity is due to interference between the non-stationary excitation and the stationary initial charge distribution. The initial state is used as the local oscillator for heterodyne amplification of the excited charge distribution to retrieve real-space movies of atomic motion on Ångstrom and femtosecond scales. This x-ray interference has not been employed to image internal motion in molecules before. Coherent vibrational motion and dispersion, dissociation, and rotational dephasing are all clearly visible in the data, thereby demonstrating the stunning sensitivity of heterodyne methods."

The novelty of the presented approach in this respect is, I think, not well introduced or discussed. It is addressed again on p. 1, right column, with The deconvolved signal is a real-space de-novo molecular movie. But this, I think, is by far too short and indirect Accessibility of this argument is limited for a broad readership in the way it is discussed in the present manuscript. This is also an example for the

aforementioned failure to clearly distinguish between what is obvious and what is new. The argument is so short and condensed that it becomes unclear what is obvious and what is new.

We get the point. Its a difficult balancing act: We were solidly hand-slapped by some of our collaboration and some local colleagues when we tried to claim outright that our method is new and not obvious. It is new and not obvious to us. All agree that no one else has made self-referencing molecular movies before. But it is also based on lots of work that nearly predicted it, all carefully referenced in the manuscript. In the end, claims of novelty are not the point of this paper. The breathtaking results speak for themselves, without our underscoring the novelty. Let the readers enjoy the paper for its results rather than its bragging rights.

Revisions: We highlight the places in the manuscript where this point is addressed: Abstract: "This x-ray interference has not been employed to image internal motion in molecules before." Second paragraph: "Here we propose and demonstrate an imaging method that employs a universal but unappreciated feature of time-resolved hard x-ray scattering that dramatically improves reconstructed images of charge motion, and enables femtosecond and sub-Ångstrom x-ray movies." Second column page 1: "The key insight in Eq. 4 is that x-ray scattering from the excited fraction in each molecule interferes with scattering from its initial state fraction, producing holographic fringes." Next paragraph and top of next column: "Previous descriptions of the formal theory of time-resolved x-ray diffraction in small molecules have not discussed the importance of this self-referenced interference [S9–S16]. Eq. 4 has been noted previously, but has not been implemented for molecular movies [S16–S19]."

Another example of this is the discussion on p. 1, left column: The method relies on the pump-probe protocol, where motion is initiated by a short start pulse, and then interrogated at a later time by a probe pulse. The pumped fraction is small, i.e. most of the molecules are not excited, Compared to the argument addressed in the paragraph above (reliance on simulations versus measured data alone) and compared to the last half sentence of this paragraph and this produces our heterodyne reference. the explanation of the pump-probe approach is by far too long (this is, I believe, well known) while the discussion of innovations and impact are too short in my view.

We have made some revisions to respond to the referee. The pump-probe discussion cannot be completely eliminated because the identification of the ground state as a holographic reference is the essential insight of this paper. Furthermore, most of the first page is now devoted to a detailed discussion of the background and novelty of this method. We particularly bring the Editor and Referee's attention to the following summary material:

Revision: "...Eq.4 differs from the result for an inhomogeneous gas mixture where there are no intramolecular cross terms and the intensity distributions of the two species simply add.

"The key insight in Eq.4 is that scattering from the excited fraction in each molecule interferes with scattering from its initial state fraction, producing holographic fringes..."

Figure 1: The intensities in the left panel are barely visible. I suggest depicting the data differently to make the measured signal more visible. I suggest including a panel/part of the figure including the time-averaged image to make accessible the size of the effect. Following this line, how about including radial cuts (intensity versus distance from center) to make accessible the intensities of the modulations? Again along the lines of making accessible the size of the effect it would be valuable to have a panel/part of the figure with the data (scattering images and cuts) at negative delays (as some sort of a control experiment).

This very detailed suggestion doesnt work well visually, and so we have rejected the specifics; but we embrace the spirit of the suggestion. Ref A also asked for quantitative explanations and so they are provided. In addition, we have added supplementary material including a full movie of the raw data, one time slice of which is in fig. 1.

Revision: The response to comment 7) by Referee A contains the new Fig. 1 and caption.

Figure 1, caption: What is CSPAD? (move explanatory info from main text to caption).

CSPAD is the Cornell-SLAC Pixel Array Detector, a 2.3 megapixel silicon array detector. This information is now in the text and the caption.

P. 2, left column: X-ray photoabsorption, though present at these x-ray energies, does not affect the fidelity because of the diffract-before-destroy principle. This is another example for where I believe the authors failed to distinguish the known from the new. What is the diffract-before-destroy principle? How is it related to X-ray photoabsorption here? The argument is very congested and hard to access.

Yes we agree, this comment has been deleted.

Figure 2, caption: What is meant with the Long- (Short-) period Q-oscillations? It appears that the distinction between long and short periods is not taken up in the main text. So what is meant? It would be necessary I think to better connect to the discussion in the main text.

This has been rewritten to make it more clear. This statement refers the intensity modulations along the Q-axis which is the vertical axis in Figure 2. The figure clearly shows both long-wavelength modulations where there is about one cycle over the whole Q-range, and also short wavelength modulations that look like ripples on the Q,t landscape.

Revision to the caption in Fig. 2: "$\beta_2(Q,t)$ as defined in Eq. 5. This term captures most of the excited state scattering signal. The time-averaged value is subtracted, and the scale is the fraction of modulation due to the holographic interference between the excited state and the reference ground state. The principal features are long-period oscillations in Q that are due to the B state, and much shorter period oscillations in Q caused by dissociation. "

P. 2, right column: This picks out scattering patterns with the symmetry of an electric dipole excitation How do the measured signals look like for parallel polarizations?

The short answer is that we didn't try to collect data with the excitation laser polarization parallel to the x-ray polarization, nor would we want to. One would not normally try parallel polarizations because this mixes up the Q-dependent intensity modulations that we are interested in with the general angle-dependence of x-ray elastic scattering. Thats why even at a synchrotron this experiment would be performed with the x-ray polarization perpendicular to the excitation dipole. And this is even more important at an FEL where the time available on the machine is severely limited, so we worked in the most favorable geometry to collect our data. This point is now made explicitly in the paper.

Revision: The paper now contains a brief discussion of polarization: "The beams have orthogonal polarizations so that the B-state wave packet, which is excited primarily in the polarization direction, will have its largest modulation along a direction where the Thomson x-ray scattering cross section is insensitive to angle."

P. 2, right column (discussion feature (a) in Figure 2): the outer turning point, approximately 4.5 A for this excitation wavelength. Is the location of the outer turning point taken from literature or extracted from the presented data? This appears to be another example of not clearly distinguishing between what is known and what is new.

The number is read right off the data plot. The calibration here is easy, since we know the scattering geometry and the laser spectrum. This is also corroborated by the dissociation velocity vector, which is tied to the excitation wavelength and the shape of the X-state. So 4.5 Angstroms is simply a description of the data in Fig. 3. However, we have also included simulations in Supplementary material. They are consistent, of course.

Revision: We have included a wave packet simulation in the Supplemental material, and also two references where the structures we can now see in the data were predicted. The revised paragraph in the main text is: "(d) Local moving peaks in the charge density are observed near the outer turning point at time delays of 0.5-0.7 ps. Similar cusp-like features in the highly dispersive upper parts of the B-state were predicted and named molecular cannons and molecular reflectrons, but they have not been observed directly before [S24, S27]."

Figure 3: Minor ticks on the x-axis in the main panel as well as in the inset seem necessary to better follow the discussion. In addition, ticks with units (energies) on the y-axis in the inset seem necessary to follow the discussion. It would be good to indicate the excitation wavelength with an arrow in the inset (accepting the relating approximations with indicating excitation in this simplified way).

We have added a scale and tick marks to the main figure and the inset in Fig.3.

Revision: Scale in Fig.3 and inset.

What is the feature ta 0.7-0.8 ps and 3.5-4 A?

The feature at 0.7-0.8ps and 3.5-4 Å is the molecular canon, as described in section (d).

Revision: We have inserted information about this feature and a reference: "(d) Local moving peaks in the charge density are observed near the outer turning point at time delays of 0.5-0.7 ps. Similar cusp-like features are predicted but have not been observed directly before [S24, S27]. [See simulation in Supplementary Materials.] "

P. 3, left column: The excitation is spread over several hundred cm-1 by thermal broadening of the initial state. In addition, the excited state wave packet is located high up in the anharmonic portion of

the B-state potential well. These conditions lead to strong dispersion, which smears the outer turning point in both space and time. It seems necessary to better distinguish between what has been known before (these conditions lead to strong dispersion, based on previous results on other molecules or on text-book knowledge?), what is assumed or known from experimental parameters (excitation is spread over several hundred cm-1 by thermal broadening of the initial state, based on simulations of the initial states of the molecules?) and what is extracted or concluded from the presented data (dispersion, which smears the outer turning point in both space and time, as visible in Figure 3?).

We think its all known before, just never seen directly. We now say this, and provide simulations.

In this same paragraph, it would be valuable to translate the spread over several hundred cm-1 to energies to directly assess the argument with the (proposed) energy scale in the inset in Figure 3.

We are not sure what this means. Perhaps it means that the reviewer does not consider cm^{-1} to be a unit of energy. Well, taken out of context thats true, but in the context of spectroscopy its a pretty standard unit of energy. But we want to be more broad-minded since we would be annoyed if a similar paper used kcal/mole units, so we will adopt eV for everything in the paper.

Revision: We have modified the following phrase in the text to include eV energy units: "The excitation is spread over several hundred cm^{-1} *($\sim$ 40 meV) by thermal broadening of the initial state."*

P. 3, left column: Discussion of feature (c): I find this very short and unclear. Try to clarify or extend.

OK. We have tried to improve this and we have also added references.

Revision of this paragraph in response to the concerns of the Referee: "There is a pulse of dissociating charge that starts near $(R, t) = (2.7\ \mathring{A}, 0)$ *and moves rapidly away from the bound region with constant velocity and only 4% of the total excited charge. The fringes recorded in Fig. 2 are sufficiently fine to show that this feature has little dispersion out to at least 16Å, well beyond the range included in Fig. 3. Its velocity is 16 Å/ps, corresponding to a kinetic energy release of approximately 0.85 eV, consistent with the separation velocity required for the molecule to dissociate into two ground-state atoms for our excitation wavelength. This prompt dissociation is consistent with transitions to a family of repulsive ungerade* states, one of which is shown in the inset in Fig. 3 [S23, S28]."

P. 3, right column, text ending with the initial strength. and starting with The method used. When reading the text I have been increasingly confused by the cross references to equations not yet shown and arguments not yet discussed and finally did not understand why the explanation for how the data in Figure 3 were extracted comes after the discussion of the data in Figure 3. I suggest swapping the related text fragments to present the results in the more classical way of results first and discussion second. The advantages (more logical, less confusing cross-referencing) seem to outweigh the disadvantages (data analysis first and exciting observations second).

In response to this suggestion, we have worked on this to make sure that equations appear when they are referred to. The reviewer is correct, this is important. As for the major re-organization of text: We have made minor changes to address this comment by the refere but we choose to leave the major elements of the orgainzation as it is for the most part, because in our opinion the impact of the paper demands that the reader understand what she is seeing before we present the data; and that she see the results before delving into the machinery of the analysis.

Revision: The scattering amplitude equation is moved in front of the others, and the paragraph that introduces it now reads as shown in response 4) of referee A.

Conclusion part, p. 4, right column: Thymine photoprotection, retinal isomerization, and cyclohexadiene ring openings are all examples of photo-initiated molecular machines that are at the core of energy conversion processes in biology, and all have been studied extensively with time-resolved spectroscopic methods. Instead of this, in my opinion, lengthy and vague discussion of photochemical effects suggest having a more interesting discussion of obstacles and challenges when applying the presented approach to more relevant systems such as multi-nuclear molecules and molecules in solution.

We like the idea of discussing whats easy and whats hard in applying this to other systems. As for mentioning three of the most heavily studied photo-assisted reactions? We think we had better at least point them out. The section has been re-written in the spirit of the referees remark.

Revision: The new conclusion reads as follows: "Self-referencing can be applied to many small molecules in liquid or gas phase. It can be valuable for photo-initiated molecular energy conversion studies such as thymine photoprotection, retinal isomerization, and cyclohexadiene ring openings, providing molecular movies at the single bond level with relevant time resolution. Pre-alignment methods can improve the measurement fidelity. The requirements are: good statistics since the excitation fraction is small; Sufficient Q-resolution to resolve single bonds; and some knowledge of the initial state charge distribution.

"Since x-ray scattering only detects charge density and motion, it cannot measure electron energies or spins. Complementary information comes from time-resolved electron and x-ray spectroscopies and photoelectron imaging [S32–S34].

"Future higher energy and higher repetition rate x-ray FELs could increase the fidelity and resolution of molecular movies. Likewise, the method could be used equally well with sub-femtosecond x-ray pulses, or with enhanced harmonic radiation from FEL undulators."

Prealignment or orientation of the initial state using strong laser fields or other methods could also improve the measurement fidelity. Why and how?

This has now been handled in references in the paper and also in the supplementary material.

---

* J.M. Glownia and A. Natan contributed equally to this work.

[S1] M. Trigo, M. Fuchs, J. Chen, M. P. Jiang, M. Cammarata, S. Fahy, D. M. Fritz, K. Gaffney, S. Ghimire, A. Higginbotham, S. L. Johnson, M. E. Kozina, J. Larsson, H. Lemke, A. M. Lindenberg, G. Ndabashimiye, F. Quirin, K. Sokolowski-Tinten, C. Uher, G. Wang, J. S. Wark, D. Zhu, and D. A. Reis, Nature Physics **9**, 790 (2013).

[S2] C. Kupitz, S. Basu, I. Grotjohann, R. Fromme, N. A. Zatsepin, K. N. Rendek, M. S. Hunter, R. L. Shoeman, T. A. White, D. Wang, D. James, J.-H. Yang, D. E. Cobb, B. Reeder, R. G. Sierra, H. Liu, A. Barty, A. L. Aquila, D. Deponte, R. A. Kirian, S. Bari, J. J. Bergkamp, K. R. Beyerlein, M. J. Bogan, C. Caleman, T.-C. Chao, C. E. Conrad, K. M. Davis, H. Fleckenstein, L. Galli, S. P. Hau-Riege, S. Kassemeyer, H. Laksmono, M. Liang, L. Lomb, S. Marchesini, A. V. Martin, M. Messerschmidt, D. Milathianaki, K. Nass, A. Ros, S. Roy-Chowdhury, K. Schmidt, M. Seibert, J. Steinbrener, F. Stellato, L. Yan, C. Yoon, T. A. Moore, A. L. Moore, Y. Pushkar, G. J. Williams, S. Boutet, R. B. Doak, U. Weierstall, M. Frank, H. N. Chapman, J. C. H. Spence, and P. Fromme, Nature **513**, 261 (2014).

[S3] M. Minitti, J. Budarz, A. Kirrander, J. Robinson, D. Ratner, T. Lane, D. Zhu, J. Glownia, M. Kozina, H. Lemke, M. Sikorski, Y. Feng, S. Nelson, K. Saita, B. Stankus, T. Northey, J. Hastings, and P. Weber, Physical Review Letters **114**, 255501 (2015).

[S4] J. Küpper, S. Stern, L. Holmegaard, F. Filsinger, A. Rouze, A. Rudenko, P. Johnsson, A. V. Martin, M. Adolph, A. Aquila, S. Bajt, A. Barty, C. Bostedt, J. Bozek, C. Caleman, R. Coffee, N. Coppola, T. Delmas, S. Epp, B. Erk, L. Foucar, T. Gorkhover, L. Gumprecht, A. Hartmann, R. Hartmann, G. Hauser, P. Holl, A. Hmke, N. Kimmel, F. Krasniqi, K.-U. Khnel, J. Maurer, M. Messerschmidt, R. Moshammer, C. Reich, B. Rudek, R. Santra, I. Schlichting, C. Schmidt, S. Schorb, J. Schulz, H. Soltau, J. C. Spence, D. Starodub, L. Strder, J. Thgersen, M. J. Vrakking, G. Weidenspointner, T. A. White, C. Wunderer, G. Meijer, J. Ullrich, H. Stapelfeldt, D. Rolles, and H. N. Chapman, Physical Review Letters **112**, 083002 (2014).

[S5] J. Yang, M. Guehr, T. Vecchione, M. S. Robinson, R. Li, N. Hartmann, X. Shen, R. Coffee, J. Corbett, A. Fry, and et al., Nature Communications **7**, 11232 (2016).

[S6] C. I. Blaga, J. Xu, A. D. DiChiara, E. Sistrunk, K. Zhang, P. Agostini, T. A. Miller, L. F. DiMauro, and C. D. Lin, Nature **483**, 194 (2012).

[S7] R. Boll, D. Anielski, C. Bostedt, J. D. Bozek, L. Christensen, R. Coffee, S. De, P. Decleva, S. W. Epp, B. Erk, and et al., Physical Review A **88**, 61402 (2013).

[S8] B. Wu, Y. Liu, C. Rose-Petruck, and G. J. Diebold, Applied Physics Letters **100**, 61110 (2012).

[S9] G. Dixit, O. Vendrell, and R. Santra, Proceedings of the National Academy of Sciences **109**, 1163611640 (2012).

[S10] M. Ben-Nun, J. Cao, and K. R. Wilson, The Journal of Physical Chemistry A **101**, 87438761 (1997).

[S11] J. Cao and K. R. Wilson, The Journal of Physical Chemistry A **102**, 9523 (1998), http://dx.doi.org/10.1021/jp982054p.

[S12] S. Bratos, F. Mirloup, R. Vuilleumier, and M. Wulff, The Journal of Chemical Physics **116**, 10615 (2002).

[S13] N. E. Henriksen and K. B. Møller, The Journal of Physical Chemistry B **112**, 558 (2008), pMID: 18052363, http://dx.doi.org/10.1021/jp075497e.

[S14] U. Lorenz, K. B. Møller, and N. E. Henriksen, Phys. Rev. A **81**, 023422 (2010).

[S15] A. Debnarova, S. Techert, and S. Schmatz, The Journal of Chemical Physics **133**, 124309 (2010).

[S16] M. Ben-Nun, T. J. Martnez, P. M. Weber, and K. R. Wilson, Chemical Physics Letters **262**, 405414 (1996).

[S17] M. Woerner, F. Zamponi, Z. Ansari, J. Dreyer, B. Freyer, M. Prmont-Schwarz, and T. Elsaesser, The Journal of Chemical Physics **133**, 64509 (2010).

[S18] M. J. J. Vrakking and T. Elsaesser, Nature Photonics **6**, 645647 (2012).

[S19] D. A. Reis and A. M. Lindenberg, "Ultrafast x-ray scattering in solids," in *Light Scattering in Solid IX*, Topics in Applied Physics, edited by M. Cardona and R. Merlin (Springer Berlin Heidelberg, 2006) p. 371422.

[S20] S. Herrmann, S. Boutet, B. Duda, D. Fritz, G. Haller, P. Hart, R. Herbst, C. Kenney, H. Lemke, M. Messerschmidt, *et al.*, Nuclear Instruments and Methods in Physics Research Section A: Accelerators, Spectrometers, Detectors and Associated Equipment **718**, 550 (2013).
[S21] See Supplemental Material at [URL will be inserted by publisher] for movies and simulations related to this experiment.
[S22] M. Chollet, R. Alonso-Mori, M. Cammarata, D. Damiani, J. Defever, J. T. Delor, Y. Feng, J. M. Glownia, J. B. Langton, S. Nelson, and et al., Journal of Synchrotron Radiation **22**, 503507 (2015).
[S23] J. Tellinghuisen, The Journal of Chemical Physics **59**, 849852 (1973).
[S24] J. L. Krause, R. M. Whitnell, K. R. Wilson, Y. Yan, and S. Mukamel, The Journal of Chemical Physics **99**, 65626578 (1993).
[S25] J. M. Budarz, M. P. Minitti, D. V. Cofer-Shabica, B. Stankus, A. Kirrander, J. B. Hastings, and P. M. Weber, Journal of Physics B: Atomic, Molecular and Optical Physics **49**, 34001 (2016).
[S26] A. Saiz-Lopez, R. W. Saunders, D. M. Joseph, S. H. Ashworth, and J. M. C. Plane, Atmos. Chem. Phys. **4**, 14431450 (2004).
[S27] H. Chen, L. Fang, V. Tagliamonti, and G. N. Gibson, Physical Review A **84**, 43427 (2011).
[S28] **55**, 10.1063/1.1675521.
[S29] D. W. Broege, R. N. Coffee, and P. H. Bucksbaum, Physical Review A **78**, 35401 (2008).
[S30] F. Rosca-Pruna and M. J. J. Vrakking, The Journal of Chemical Physics **116**, 65796588 (2002).
[S31] F. Rosca-Pruna and M. J. J. Vrakking, Physical Review Letters **87**, 153902 (2001).
[S32] A. Stolow, A. E. Bragg, and D. M. Neumark, Chem. Rev. **104**, 1719 (2004).
[S33] T. Suzuki, Annual Review of Physical Chemistry **57**, 555 (2006).
[S34] B. K. McFarland, J. P. Farrell, S. Miyabe, F. Tarantelli, A. Aguilar, N. Berrah, C. Bostedt, J. D. Bozek, P. H. Bucksbaum, J. C. Castagna, and et al., Nature Communications **5**, 4235 (2014).